Representing Graphs by Polygons with Edge Contacts in 3D*

Elena Arseneva[1], Linda Kleist[2], Boris Klemz[3], Maarten Löffler[4], André Schulz[5], Birgit Vogtenhuber[6], and Alexander Wolff[7]

1 **Saint Petersburg State University, Russia**
`e.arseneva@spbu.ru`

2 **Technische Universität Braunschweig, Germany**
`kleist@ibr.cs.tu-bs.de`

3 **Freie Universität Berlin, Germany**
`klemz@inf.fu-berlin.de`

4 **Utrecht University, the Netherlands**
`m.loffler@uu.nl`

5 **FernUniversität in Hagen, Germany**
`andre.schulz@fernuni-hagen.de`

6 **Technische Universität Graz, Austria**
`bvogt@ist.tugraz.at`

7 **Universität Würzburg, Germany**
`orcid.org/0000-0001-5872-718X`

Abstract

A graph has an edge-contact representation with polygons if its vertices can be represented by interior-disjoint polygons such that two polygons share a common edge if and only if the corresponding vertices are adjacent. In this work we study representations in 3D.

We show that every graph has an edge-contact representation with polygons in 3D, while this is not the case if we additionally require that the polygons are convex. In particular, we show that every graph containing K_5 as a subgraph does not admit a representation with convex polygons. On the other hand, $K_{4,4}$ admits such a representation, and so does every K_n where every edge is subdivided by a vertex. We also construct an infinite family (G_n) of graphs where G_n has n vertices, $6n - o(n)$ edges, and admits an edge-contact representation with convex polygons in 3D.

Lines 174

1 Introduction

A graph has a contact representation if its vertices can be represented by interior-disjoint geometric objects such that two objects touch exactly if the corresponding vertices are adjacent. In concrete settings, one usually restricts the set of geometric objects (circles, lines, polygons, ...), the type of contact, and the embedding space. Numerous results about which graphs admit a contact representation of some type are known. Giving a comprehensive overview is out of scope for this extended abstract. We therefore mention only few results. By the Andreev–Koebe–Thurston circle packing theorem [3, 20] every planar graph has a contact representation by touching disks in 2D. Contact representations of graphs in 2D

* B.V. partially supported by the Austrian Science Fund within the collaborative DACH project *Arrangements and Drawings* as FWF project I 3340-N35; A.W. acknowledges support by DFG project WO 758/9-1. This work has been initiated at the Dagstuhl Seminar 19352 “Computation in Low-Dimensional Geometry and Topology”. We thank all the participants for the great atmosphere and fruitful discussions.

36th European Workshop on Computational Geometry, Würzburg, Germany, March 16–18, 2020.
This is an extended abstract of a presentation given at EuroCG’20. It has been made public for the benefit of the community and should be considered a preprint rather than a formally reviewed paper. Thus, this work is expected to appear eventually in more final form at a conference with formal proceedings and/or in a journal.

have since been considered for quite a variety of shapes, including triangles [4, 8, 13, 14, 19], axis-aligned rectangles [1, 5, 11], curves [15], or line segments [6, 7, 16] in 2D and balls [17], tetrahedra [2] or cubes [12, 18] in 3D. Evans et al. [10] showed that every graph has a contact representation in 3D in which each vertex is represented by a convex polygon and two polygons touch *in a corner* if and only if the corresponding two vertices are adjacent.

In this work we study contact representations with polygons in 3D where a contact between two polygons is realized by sharing a proper edge that is not part of any other polygon of the representation. The special case where we require that the polygons are convex is of particular interest. Note that we do not require that the polyhedral complex induced by the contact representation is a closed surface. In particular, not every polygon edge has to be in contact with another polygon. By Steinitz's theorem [21], every 3-connected planar graph can be realized as a convex polyhedron, whose dual is also a planar graph. Thus all planar graphs have such a representation with convex polygons.

Results. We show that for the case of nonconvex polygons, every graph has an edge-contact representation in 3D. For convex polygons, the situation is more intricate. We show that certain graphs do not have such a representation (even some 3-trees). On the other hand, many nonplanar graphs (for example, $K_{4,4}$) have such a representation. In particular, graphs that admit an edge-contact representation with convex polygons in 3D can be considerably denser than planar graphs.

2 Representations with General Polygons

First we show that every graph can be represented by nonconvex polygons; see Figure 1.

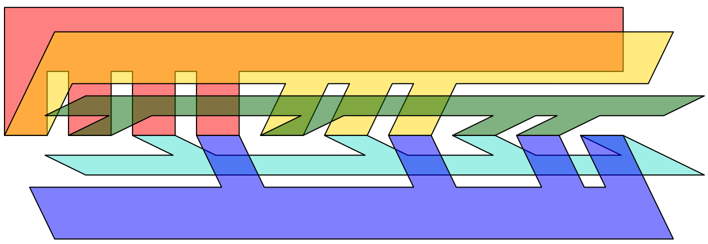

Figure 1 A realization of K_5 by nonconvex polygons with edge contacts in 3D.

▶ **Proposition 2.1.** *Every graph can be realized by polygons with edge contacts in 3D.*

Proof. To represent a graph G with n vertices, we start with n rectangles such that the intersection of all these rectangles is a line segment s. We then cut away parts of each rectangle thereby turning it into a comb-shaped polygon as illustrated in Figure 1. This step ensures that for each pair (P, P') of polygons, there is a subsegment s' of s such that s' is an edge of both P and P' that is disjoint from the remaining polygons. The result is a representation of K_n. To obtain a realization of G, it remains to remove edge contacts that correspond to unwanted adjacencies, which is easy. ◀

If we additionally insist that each polygon shares all of its edges with other polygons, the polygons describe a closed volume. In this model, K_7 can be realized as the Szilassi polyhedron; see Figure 2. The tetrahedron and the Szilassi polyhedron are the only two known polyhedra in which each face shares an edge with each other face [22]. Which other graphs can be represented in this way remains an open problem.

Figure 2 The Szilassi polyhedron realizes K_7 by nonconvex polygons with edge contacts in 3D [22].

3 Representations with Convex Polygons

We now consider the setting where each vertex of the given graph is represented by a convex polygon in 3D and two vertices of the given graph are adjacent if and only if their polygons intersect in a common edge. (In most previous work, it was only required that the edge of one polygon is contained in the edge of the adjacent polygon. For example, Duncan et al. [9] showed that in this model every planar graph can be realized by hexagons in the plane and that hexagons are sometimes necessary.) Note that it is allowed to have edges that do not touch other polygons. Further, non-adjacent polygons may intersect at most in a common vertex. We start with some simple observations.

▶ **Proposition 3.1.** *Every planar graph can be realized by convex polygons with edge contacts in 2D.*

Proof. Let G be a planar (embedded) graph with at least three vertices (for at most two vertices the statement is trivially true). Add to G a new vertex r and connect it to all vertices of some face. Let G' be a triangulation of the resulting graph. Then the dual $G^\star$ of G' is a cubic 3-connected planar graph. Using Tutte's barycentric method, draw $G^\star$ into a regular polygon with $\deg_{G'}(r)$ corners such that the face dual to r becomes the outer face. Note that the interior faces in this drawing are convex polygons. Hence the drawing is an edge-contact representation of $G' - r$. To convert it to a representation of G, we may need to remove some edge contacts, which can be easily achieved. ◀

Note that Proposition 3.1 also follows directly from the Andreev–Koebe–Thurston circle packing theorem. So for planar graphs vertex and edge contacts behave similarly. For nonplanar graphs (for which we need the third dimension), the situation is different. Here, edge contacts are more restrictive. We introduce the following notation. In a 3D representation of a graph G by polygons, we denote by P_v the polygon that represents vertex v of G.

▶ **Lemma 3.2.** *Let G be a graph. Consider a 3D edge-contact representation of G with convex polygons. If G contains a triangle uvw, polygons P_v and P_w lie on the same side of the plane that supports P_u.*

Proof. Due to the convexity of the polygons, P_v and P_w either both lie above or both lie below the plane that supports P_u, otherwise P_v and P_w cannot share an edge. In this case, the edge vw of G would not be represented; a contradiction. ◀

▶ **Proposition 3.3.** *For $n \geq 5$, K_n is not realizable by convex polygons with edge contacts in 3D.*

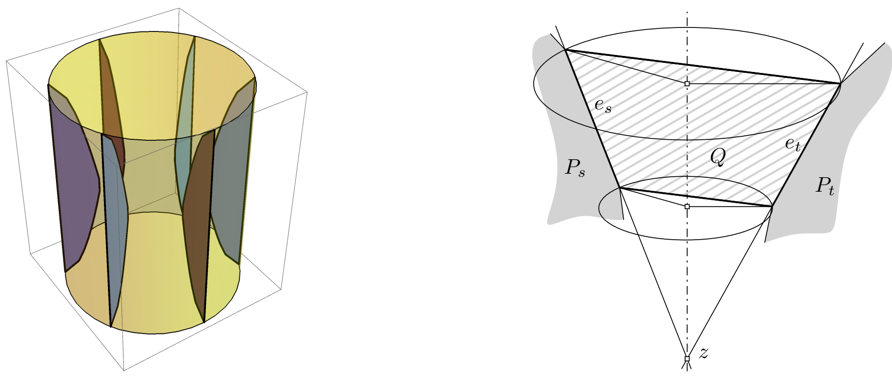

(a) The arrangement of the polygons $P_1, \ldots, P_n$. **(b)** Quadrilateral Q spanned by e_s and e_t.

Figure 3 Illustration for the proof of Proposition 3.4.

Proof. Assume that K_n admits a 3D edge-contact representation. Since every three vertices in K_n are pairwise connected, by Lemma 3.2, for every polygon of the representation, its supporting plane has the remaining polyhedral complex on one side. In other words, the complex we obtain is a subcomplex of a convex polyhedron. Consequently, the dual graph has to be planar, which rules out K_n for $n \geq 5$. ◀

► **Proposition 3.4.** *Let K'_n be the subdivision of the complete graph K_n in which every edge is subdivided with one vertex. For every n, K'_n has an edge contact representation with convex polygons in 3D.*

Proof sketch. For $n \leq 4$ the statement is true by Proposition 3.1. We sketch the construction of a representation for $n \geq 5$; see Figure 3. Let P be a convex polygon with $k = 2\binom{n}{2}$ vertices, called $v_1, v_2, \ldots, v_k$, such that v_1v_k is a long edge and the remaining vertices form a flat convex chain connecting v_1 and v_k. We represent each high-degree vertex of K'_n by a copy of P. We arrange those copies in pairwise different vertical planes containing the z-axis such that all copies of v_1v_k are arranged vertically at the same height and at the same distance from the z-axis; and such that the convex chain of each copy of P faces the z-axis but does not intersect it. Consider two different copies P_s and P_t of P in this arrangement. They contain copies e_s and e_t of the same edge e of P. It can be shown that e_s and e_t are coplanar. Moreover, they form a convex quadrilateral Q that does not intersect the arrangement except in e_s and e_t. We arbitrarily assign each edge $v_{2i-1}v_{2i}$, $1 \leq i \leq k/2 = \binom{n}{2}$, to some edge st of K_n and use the quadrilateral Q spanned by e_s and e_t to represent the subdivision vertex of st in K'_n. As any two such quadrilaterals are vertically separated and hence disjoint, those $\binom{n}{2}$ quadrilaterals together with the n copies of P constitute a valid representation of K'_n. ◀

► **Proposition 3.5.** *$K_{4,4}$ is realizable by convex polygons with edge contacts in 3D.*

Proof sketch. We sketch how to obtain a realization. Start with a box in 3D and intersect it with two rectangular slabs as indicated in Figure 4 on the left. We can now draw polygons on the faces of this complex such that every vertical face contains a polygon that has an edge contact with a polygon on a horizontal or slanted face. The polygons on the slanted faces lie in the interior of the box and intersect each other. To remove this intersection, we pull out one corner of the original box; see Figure 4. ◀

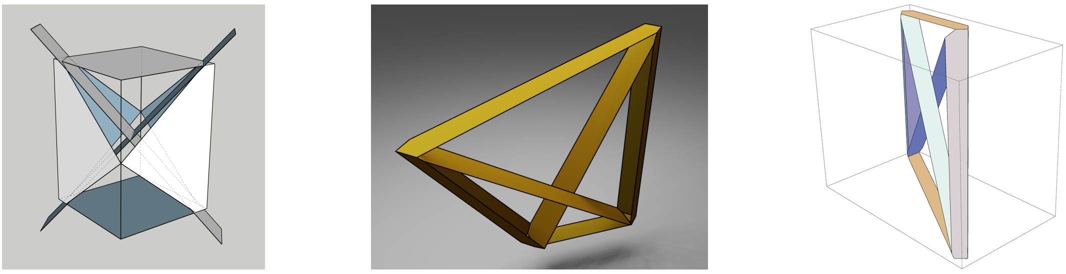

Figure 4 A realization of $K_{4,4}$ by convex polygons with edge contacts in 3D.

In contrast to Proposition 3.5, we believe that the analogous statement does not hold for all bipartite graphs, i.e., we conjecture the following:

▶ **Conjecture 3.6.** *There exist values n and m such that the complete bipartite graph $K_{m,n}$ is not realizable by convex polygons with edge contacts in 3D.*

By Proposition 3.1, all planar 3-trees can be realized by convex polygons with edge contacts (even in 2D). When switching to 3D, also nonplanar 3-trees can have a realization by convex polygons with edge contacts; see for example Figure 5. However, this is not the case for all nonplanar 3-trees.

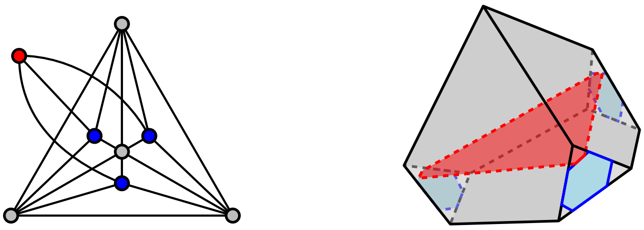

Figure 5 A nonplanar 3-tree with a realization by convex polygons with edge contacts in 3D. The gray vertices form a K_4.

▶ **Proposition 3.7.** *Not all 3-trees can be realized by convex polygons with edge contacts in 3D.*

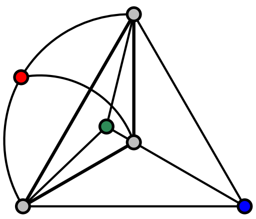

(a) A 3-tree that is not realizable by convex polygons with edge contacts in 3D. The gray vertices form a 3-cycle.

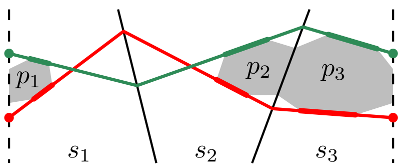

(b) Schematic drawing of a potential realization. Net of the three gray polygons and traces of the planes that contain the red and green polygons, which must touch each of the gray polygons. The line of intersection between two of the gray polygons is drawn twice (dashed).

Figure 6 Illustrations for the proof of Proposition 3.7.

Proof sketch. We claim that the 3-tree in Figure 6a, which consists of $K_{3,3}$ plus a cycle that connects the gray vertices of one part of the bipartition does not have a representation with convex polygons. The details are presented in the appendix. ◀

It is an intriguing question how dense graphs that admit an edge-contact representation with convex polygons in 3D can be. In contrast to the results for corner contacts [10] and nonconvex polygons (Proposition 2.1) in 3D, we could not find a construction with a superlinear number of edges. The following construction yields the densest graphs we know.

▶ **Theorem 3.8.** *There is an unbounded family of graphs that admit edge-contact representations with convex polygons in 3D and have the property that a graph with n vertices has $6n - o(n)$ edges.*

Proof sketch. We first construct a contact representation of $m = \lceil \sqrt{n} \rceil$ regular octagons arranged as in a truncated square tiling; see Figure 7(a). Since the underlying geometric graph of the tiling is a Delaunay tessellation, we can lift the points to the paraboloid such that each octagon is lifted to coplanar points. We call the corresponding (scaled and rotated) polyhedral complex Γ; see Figure 7(b). Next we place $\lfloor \sqrt{n} \rfloor$ copies of Γ in a cyclic fashion as

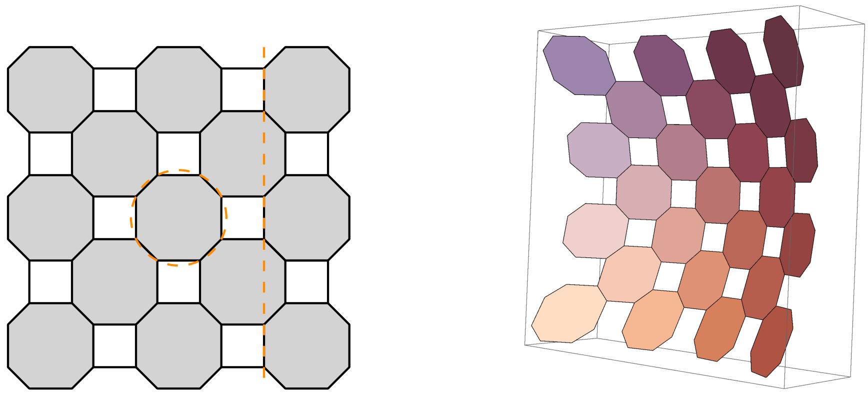

(a) The plane octagon structure. **(b)** The complex Γ.

Figure 7 Proof of Theorem 3.8: construction of the complex Γ.

shown in Figure 8(a) and we add vertical polygons in to generate a contact with the $\sqrt{m}$ vertical edges of the octagons; see Figure 8(b). To connect the horizontal edges, we use the

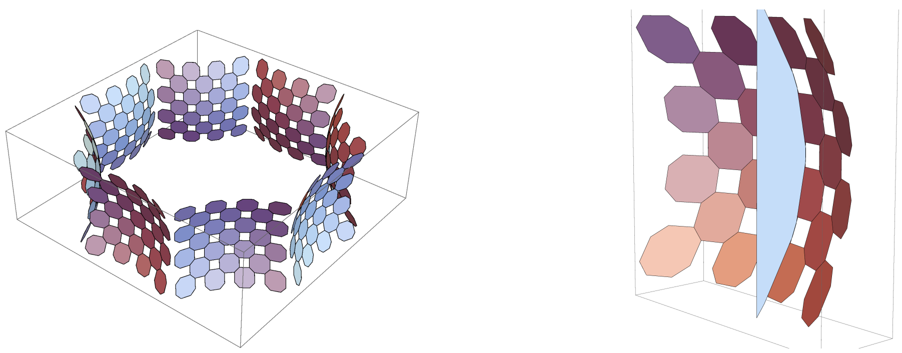

(a) The placement of the copies of Γ. **(b)** One vertical polygon.

Figure 8 Proof of Theorem 3.8: placement of the copies of Γ and vertical polygons.

"inner space" of our construction as illustrated in Figure 9(a). Finally, a slight perturbation fixes the following two issues: First, many of the horizontal polygons lie on the same plane and intersect each other. Second, many edges of vertical polygons run along the faces of Γ. To fix these problems we modify the initial grid slightly; see Figure 9(b). ◀

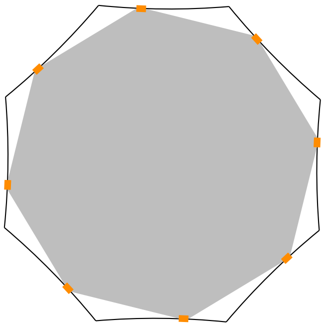

(a) The location of a horizontal polygon as seen in a cross section.

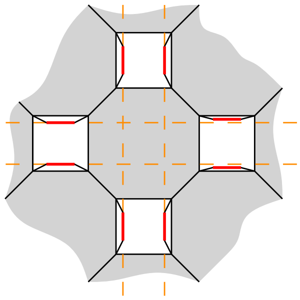

(b) The modifications for Γ to separate nondisjoint faces.

Figure 9 Proof of Theorem 3.8: horizontal polygons and final modifications.

4 Conclusion and Open Problems

An application of Turán's theorem [23] with Proposition 3.3 implies that the maximum number $e_{\mathrm{cp}}(n)$ of edges in an n-vertex graph that admits an edge contact representation with convex polygons is at most $\frac{3}{8}n^2$. Theorem 3.8 gives a lower bound of $6n - o(n)$ for $e_{\mathrm{cp}}(n)$. We tend to believe that the latter is closer to the truth than the former and conclude with the following open problem.

▶ **Question 4.1.** *What is the maximum number $e_{\mathrm{cp}}(n)$ of edges that an n-vertex graph admitting an edge contact representation with convex polygons can have?*

References

1. Md. Jawaherul Alam, Therese C. Biedl, Stefan Felsner, Andreas Gerasch, Michael Kaufmann, and Stephen G. Kobourov. Linear-time algorithms for hole-free rectilinear proportional contact graph representations. *Algorithmica*, 67(1):3–22, 2013. doi:10.1007/s00453-013-9764-5.
2. Md. Jawaherul Alam, Muriel Dulieu, Justin Iwerks, and Joseph O'Rourke. Tetrahedron contact graphs. In *Fall Workshop Comput. Geom.*, 2013.
3. E. M. Andreev. Convex polyhedra in Lobačevskiĭ spaces. *Mat. Sb. (N.S.)*, 81 (123)(3):445–478, 1970. doi:10.1070/SM1970v010n03ABEH001677.
4. Melanie Badent, Carla Binucci, Emilio Di Giacomo, Walter Didimo, Stefan Felsner, Francesco Giordano, Jan Kratochvíl, Pietro Palladino, Maurizio Patrignani, and Francesco Trotta. Homothetic triangle contact representations of planar graphs. In Prosenjit Bose, editor, *Proc. Canadian Conf. Comput. Geom. (CCCG'07)*, pages 233–236, 2007. URL: http://cccg.ca/proceedings/2007/09b4.pdf.
5. Adam L. Buchsbaum, Emden R. Gansner, Cecilia M. Procopiuc, and Suresh Venkatasubramanian. Rectangular layouts and contact graphs. *ACM Trans. Algorithms*, 4(1), 2008. doi:10.1145/1328911.1328919.

6 Hubert de Fraysseix, P Ossona de Mendez, and János Pach. Representation of planar graphs by segments. *Intuitive Geometry*, 63:109–117, 1991.

7 Hubert de Fraysseix and Patrice Ossona de Mendez. Representations by contact and intersection of segments. *Algorithmica*, 47(4):453–463, 2007. `doi:10.1007/s00453-006-0157-x`.

8 Hubert de Fraysseix, Patrice Ossona de Mendez, and Pierre Rosenstiehl. On triangle contact graphs. *Combinatorics, Probability and Computing*, 3:233–246, 1994. `doi:10.1017/S0963548300001139`.

9 Christian A. Duncan, Emden R. Gansner, Y. F. Hu, Michael Kaufmann, and Stephen G. Kobourov. Optimal polygonal representation of planar graphs. *Algorithmica*, 63(3):672–691, 2012. `doi:10.1007/s00453-011-9525-2`.

10 William Evans, Paweł Rzążewski, Noushin Saeedi, Chan-Su Shin, and Alexander Wolff. Representing graphs and hypergraphs by touching polygons in 3D. In Daniel Archambault and Csaba Tóth, editors, *Proc. Graph Drawing & Network Vis. (GD'19)*, volume 11904 of *LNCS*, pages 18–32. Springer, 2019. URL: `http://arxiv.org/abs/1908.08273`, `doi:10.1007/978-3-030-35802-0_2`.

11 Stefan Felsner. Rectangle and square representations of planar graphs. In János Pach, editor, *Thirty Essays on Geometric Graph Theory*, pages 213–248. Springer, 2013.

12 Stefan Felsner and Mathew C. Francis. Contact representations of planar graphs with cubes. In Ferran Hurtado and Marc J. van Kreveld, editors, *Proc. 27th Ann. Symp. Comput. Geom. (SoCG'11)*, pages 315–320. ACM, 2011. `doi:10.1145/1998196.1998250`.

13 Emden R. Gansner, Yifan Hu, and Stephen G. Kobourov. On touching triangle graphs. In Ulrik Brandes and Sabine Cornelsen, editors, *Proc. Graph Drawing (GD'10)*, volume 6502 of *LNCS*, pages 250–261. Springer, 2010. `doi:10.1007/978-3-642-18469-7`.

14 Daniel Gonçalves, Benjamin Lévêque, and Alexandre Pinlou. Triangle contact representations and duality. *Discrete Comput. Geom.*, 48(1):239–254, 2012. `doi:10.1007/s00454-012-9400-1`.

15 Petr Hliněný. Classes and recognition of curve contact graphs. *J. Combin. Theory Ser. B*, 74(1):87–103, 1998.

16 Petr Hliněný. Contact graphs of line segments are NP-complete. *Discrete Math.*, 235(1):95–106, 2001. `doi:10.1016/S0012-365X(00)00263-6`.

17 Petr Hliněný and Jan Kratochvíl. Representing graphs by disks and balls (a survey of recognition-complexity results). *Discrete Math.*, 229(1–3):101–124, 2001. `doi:10.1016/S0012-365X(00)00204-1`.

18 Linda Kleist and Benjamin Rahman. Unit contact representations of grid subgraphs with regular polytopes in 2D and 3D. In Christian Duncan and Antonios Symvonis, editors, *Proc. Graph Drawing (GD'14)*, volume 8871 of *LNCS*, pages 137–148. Springer, 2014. `doi:10.1007/978-3-662-45803-7_12`.

19 Stephen G. Kobourov, Debajyoti Mondal, and Rahnuma Islam Nishat. Touching triangle representations for 3-connected planar graphs. In Walter Didimo and Maurizio Patrignani, editors, *Proc. Graph Drawing (GD'12)*, volume 7704 of *LNCS*, pages 199–210. Springer, 2013. `doi:10.1007/978-3-642-36763-2\_18`.

20 Paul Koebe. Kontaktprobleme der konformen Abbildung. *Berichte über die Verhandlungen der Sächsischen Akad. der Wissen. zu Leipzig. Math.-Phys. Klasse*, 88:141–164, 1936.

21 Ernst Steinitz. Polyeder und Raumeinteilungen. In *Encyclopädie der mathematischen Wissenschaften*, volume 3-1-2 (Geometrie), chapter 12, pages 1–139. B. G. Teubner, Leipzig, 1922.

22 Szilassi polyhedron. Wikipedia entry. Accessed 2019-10-08. URL: `https://en.wikipedia.org/wiki/Szilassi_polyhedron`.

23 Paul Turán. Eine Extremalaufgabe aus der Graphentheorie. *Mat. Fiz. Lapok*, 48:436–452, 1941.

A Appendix: Remaining Details of Section 3

▶ **Proposition 3.4.** *Let K'_n be the subdivision of the complete graph K_n in which every edge is subdivided with one vertex. For every n, K'_n has an edge contact representation with convex polygons in 3D.*

Proof. It is clear that the proposition holds for $n \in \{1, 2\}$. We now show it for $n \geq 3$.

Let P be a convex polygon with $k = 2\binom{n}{2}$ vertices $v_1, v_2, \ldots, v_k$ in the plane. Assume that v_1 and v_k lie on the x-axis and that the rest of the polygon is a convex chain that projects vertically onto the line segment $\overline{v_1 v_k}$, which we call the *long edge* of P. We call the other edges *short edges*. We choose P such that no short edge is parallel to $\overline{v_1 v_k}$.

For the n high degree vertices in K'_n, we take n copies $P_1, \ldots, P_n$ of P and place them in 3D such that their long edges lie on the vertical boundary of a cylinder Z that has the z-axis as center; see Figure 10(a). For $s = 1, 2, \ldots, n$, each polygon P_s lies on a distinct halfplane that is bounded by the z-axis, and all polygons lie inside the cylinder Z. Finally, all polygons are positioned at the same height, implying that for any vertex v_j of P, all copies of v_j lie in a horizontal plane h_i and have the same distance to the z-axis.

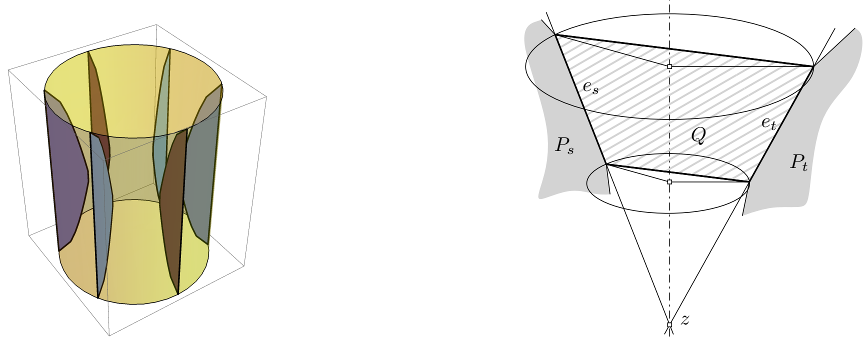

(a) The arrangement of the polygons $P_1, \ldots, P_n$. **(b)** Quadrilateral Q spanned by e_s and e_t.

Figure 10 Illustration for the proof of Proposition 3.4.

Let $i \in \{1, 2, \ldots, k-1\}$. Then the edge $e = v_i v_{i+1}$ is a short edge of P. For $s = 1, 2, \ldots, n$, we denote by e_s and v_i^s the appearance of e and v_i in P_s, respectively. We claim that, for $1 \leq s < t \leq n$, the edges e_s and e_t span a convex quadrilateral that does not intersect any P_j with $j \notin \{s, t\}$. To prove the claim, we argue as follows.

By the positioning of P_s and P_t inside Z, the supporting lines of e_s and e_t intersect at a point z on the z-axis, implying that e_s and e_t are coplanar. Moreover, v_i^s and v_i^t are at the same distance from z, and the same holds for v_{i+1}^s and v_{i+1}^t. Hence the triangle spanned by z, v_i^s, and v_i^t is similar to the triangle spanned by z, v_{i+1}^s, and v_{i+1}^t, implying that $v_i^s v_i^t$ and $v_{i+1}^s v_{i+1}^t$ are parallel and hence span a convex quadrilateral Q. Finally, no polygon P_j with $j \notin \{s, t\}$ can intersect Q as any point in the interior of Q lies closer to the z-axis as any point of P_j at the same z-coordinate, which proves the claim.

We arbitrarily assign each edge $v_{2i-1} v_{2i}$, $1 \leq i \leq k/2$ to some edge st of K_n. By our claim, the edge e_s of P_s and the edge e_t of P_t span a convex quadrilateral Q that does not intersect any P_j with $j \notin \{s, t\}$. We use Q as polygon for the subdivision vertex of the edge st in K'_n. The quadrilateral Q lies in the horizontal slice of Z bounded by the horizontal planes h_{2i-1} and h_{2i} for some $1 \leq i \leq k/2$. Since any two such slices are are vertically separated and hence disjoint, the $\binom{n}{2}$ quadrilaterals together with the n copies of P constitute a valid representation of K'_n. ◀

▶ **Proposition 3.7.** *Not all 3-trees can be realized by convex polygons with edge contacts in 3D.*

Proof. Consider the 3-tree in Figure 11a, which consists of $K_{3,3}$ plus a cycle that connects the gray vertices of one part of the bipartition. The other part of the bipartition consists of three colored vertices (red, green, blue). For the sake of contradiction, assume that there is a representation by convex polygons with edge contacts and distinguish two cases: Either the three polygons are coplanar or not.

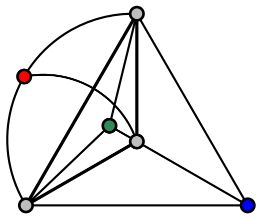

(a) A 3-tree that is not realizable by convex polygons with edge contacts in 3D. The gray vertices form a 3-cycle.

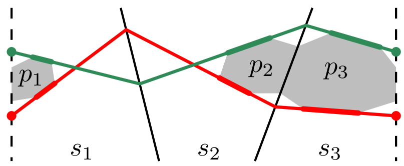

(b) Schematic drawing of a potential realization. Net of the three gray polygons and traces of the planes that contain the red and green polygons, which must touch each of the gray polygons. The line of intersection between two of the gray polygons is drawn twice (dashed).

Figure 11 Illustrations for the proof of Proposition 3.7.

If the gray polygons are coplanar, then all edge contacts must lie in the same plane. This, however, contradicts the fact that $K_{3,3}$ is not planar.

If the three edges are not coplanar, the gray polygons form a prism-like shape. Note that every colored vertex together with the gray vertices forms a K_4. Hence, by Lemma 3.2, all gray polygons must lie on one side of the supporting plane of a colored polygon. Each supporting plane of a colored polygon intersects the gray triangular prism in a triangle. Two of these triangles must intersect (otherwise one of the outer colored polygons would be cut off by the middle colored polygon and would not have any contact with the gray polygons). The two intersecting triangles (say, the red and the green) cross each other exactly twice, and the two points of intersection lie on two distinct sides s_1 and s_2 of the gray prism; see Figure 11b. Let s_3 denote the side of the gray prism that does not contain any of these intersection points. Each of the two crossing triangles intersects s_3 in a line segment. These two line segments partition s_3 into three regions. For $i \in \{1, 2, 3\}$, let p_i denote the gray polygon that lies on side s_i. Polygon p_3 lies in the middle (bounded) region of s_3, otherwise it cannot have an edge contact with both the red and the green polygon. The two crossing triangles partition each of the remaining two sides s_1 and s_2 into four regions. Two of these regions are unbounded; the other two are bounded and triangular. To realize edge contacts with p_3, polygons p_1 and p_2 have to be located in the triangular region of s_1 and s_2, respectively, that is adjacent to the middle region of s_3. However, in this case p_1 and p_2 cannot possibly touch; a contradiction. ◀

▶ **Theorem 3.8.** *There is an unbounded family of graphs that admit edge-contact representations with convex polygons in 3D and have the property that a graph with n vertices has $6n - o(n)$ edges.*

Proof. We give a construction with respect for constructing G_i for which we can make the graphs arbitrarily large. Instead of specifying the graph we will describe the contact representation (the dual). We will leave out a few details and discuss the general idea first, before giving the actual construction. In particular, some of the polygons might first have an intersection that is not a common edge.

Pick some number n. Note that in the end the total number of faces will exceed n, but only by $o(n)$. We start with constructing a representation that has $m = \lceil \sqrt{n} \rceil$ faces. The faces are arranged as the regular octagons in a truncated square tiling; see Figure 12(a). We choose the grid dimension such that height and width are equal. For this we fill up the last row/column with extra octagons exceeding m if needed. Note that we only consider the octagons and leave the quadrilaterals as holes. The underlying geometric graph of the tiling is a Delaunay tessellation, which can be easily checked by the empty-circle-property. As a consequence we can lift the points to the paraboloid such that each octagon is lifted to coplanar points. We call the corresponding polyhedral complex Γ. For convenience we scale the height of Γ down and rotate such it "stands upright" as shown in Figure 12(b).

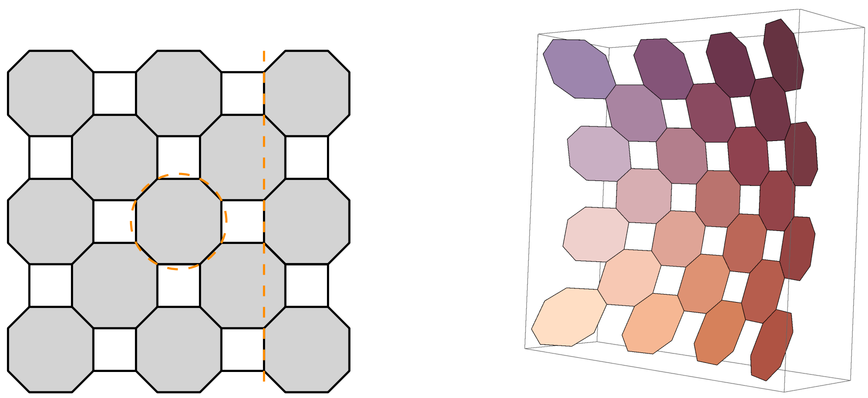

(a) The plane octagon structure. **(b)** The complex Γ.

Figure 12 Proof of Theorem 3.8: construction of the complex Γ.

Next we make $\lfloor \sqrt{n} \rfloor$ copies of Γ and place them in a cyclic fashion as shown in Figure 13(a). To finish the construction we add further polygons. These polygons attach to the holes in every copy of Γ. Every hole is a quadrilateral with two (nearly) vertical and two horizontal edges. To generate an adjacency with the vertical edges we add vertical polygons. Note that in the initial plane tiling, the $2m$ vertical edges lie on roughly $2\sqrt{m}$ lines. Hence, in Γ, each of these lines defines a vertical plane and the contained edges of the quadrilateral are part of a convex chain. As a consequence we can add vertical polygons in every of these planes to generate a contact with the vertical edges; see Figure 13(b).

We are left with connecting the horizontal edges. For this we use the "inner space" of our construction. Pick one edge of Γ. The copies of that edge in the other copies of Γ lie on a horizontal plane. Further, if we have scaled properly, these edges span a convex polygon as shown in Figure 14(a).

We have ignored two issues, which we will fix now. First, many of the horizontal polygons lie on the same plane and intersect each other. Second, many edges of vertical polygons run along the faces of Γ. To fix these problems we modify the initial grid slightly. Every octagon is replaced by a convex 16-gon by adding a 2-vertex chain on every horizontal and vertical edge. We call the inner edges of the 2-chains *connectors*. Every connector has a corresponding octagon edge it overarches. If the corresponding edge is a horizontal edge in Γ we call the connector *horizontal*; otherwise *vertical*. All connectors will be placed such that they are parallel to their corresponding octagon edges. We make sure that if a set of vertical

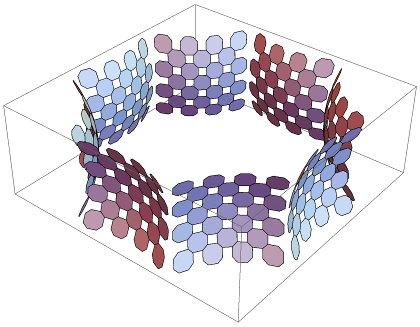

(a) The placement of the copies of Γ.

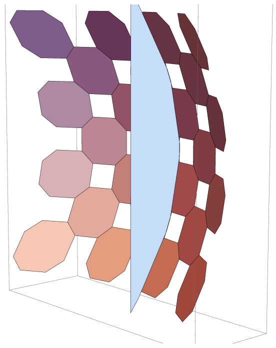

(b) One vertical polygon.

Figure 13 Proof of Theorem 3.8: placement of the copies of Γ and vertical polygons.

edges were on a common line then also their vertical connectors lie on a common line. On the other hand we make sure that none of the horizontal connectors lie on a common line; see Figure 14(b). For the modified plane embedding we use now the same lifting as before, which means that every 16-gon is lifted to the same plane as its corresponding octagon. Our modification has achieved the following. The planes spanned by a (lifted) horizontal connector and its copies are all horizontal but disjoint. The (lifted) vertical connectors of vertical edges that belonged to a vertical polygon lie on a common plane and the connectors span a convex polygon that does not intersect the interior of faces in Γ. As a consequence we can establish the horizontal and vertical polygons at the connectors to get the same connectivity as before, but the face interiors are disjoint.

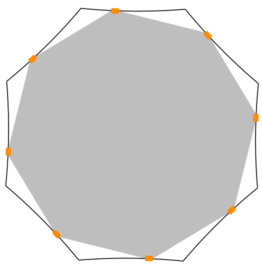

(a) The location of a horizontal polygon as seen in a cross section.

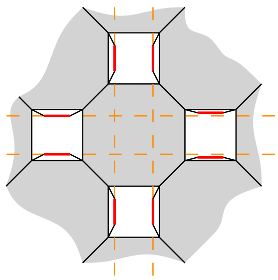

(b) The modifications for Γ to separate nondisjoint faces.

Figure 14 Proof of Theorem 3.8: horizontal polygons and final modifications.

As the last step we bound the edges of the dual graph of the constructed structure, i.e., we count the number of face-adjacencies in the polyhedral complex. For convenience we refer to the complex with the octagons, since it has the same incidences. Note that we have n octagons but only $O(n/m) = O(m)$ horizontal and $O(m\sqrt{m})$ vertical polygons. For n' being the total number of faces, we have $o(n')$ faces that are not octagons. Ignore the octagons on the boundary of Γ for now. Every octagon has 8 neighbors, 4 of them with other octagons. This implies that in total we have $6n$ adjacencies (when adding up, the octagon–octagon adjacencies are counted twice). The octagon edges on the boundary of Γ and its copies have fewer adjacencies, but there are only $O(m\sqrt{m})$ many of them. Hence, in total we have only $o(n)$ of them. Consequently, most of the n' faces are octagons with 8 neighbors and only $o(n')$ faces are different. This yields $6n' - o(n')$ adjacencies as stated. ◀